



Contents lists available at ScienceDirect

Journal of Rock Mechanics and Geotechnical Engineering

journal homepage: www.rockgeotech.org

Full Length Article

Attenuation of rock blasting induced ground vibration in rock-soil interface

Bhagya Jayasinghe^a, Zhiye Zhao^{a,*}, Anthony Goh Teck Chee^a, Hongyuan Zhou^b, Yilin Gui^c

^aSchool of Civil and Environmental Engineering, Nanyang Technological University, Singapore

^bKey Laboratory of Urban Security and Disaster Engineering of Ministry of Education, Beijing University of Technology, Beijing, China

^cSchool of Civil Engineering and Geosciences, Newcastle University, Newcastle upon Tyne, UK

ARTICLE INFO

Article history:

Received 8 July 2018

Received in revised form

3 November 2018

Accepted 24 December 2018

Available online xxx

Keywords:

Rock blasting

Field tests

Blast wave propagation

Peak particle velocity (PPV)

Rock-soil interface

ABSTRACT

Blasting has been widely used in mining and construction industries for rock breaking. This paper presents the results of a series of field tests conducted to investigate the ground wave propagation through mixed geological media. The tests were conducted at a site in the northwestern part of Singapore composed of residual soil and granitic rock. The field test aims to provide measurement data to better understand the stress wave propagation in soil/rock and along their interface. Triaxial accelerometers were used for the free field vibration monitoring. The measured results are presented and discussed, and empirical formulae for predicting peak particle velocity (PPV) attenuation along the ground surface and in soil/rock were derived from the measured data. Also, the ground vibration attenuation across the soil-rock interface was carefully examined, and it was found that the PPV of ground vibration was decreased by 37.2% when it travels from rock to soil in the vertical direction.

© 2019 Institute of Rock and Soil Mechanics, Chinese Academy of Sciences. Production and hosting by Elsevier B.V. This is an open access article under the CC BY-NC-ND license (<http://creativecommons.org/licenses/by-nc-nd/4.0/>).

1. Introduction

In view of Singapore's rapid development and land scarcity, extensive studies are currently being undertaken to consider how to create extra space for residential, commercial and industrial use. Various methods and approaches for balancing efficiency and economical aspects are being considered to create more space, depending on Singapore's unique geological characteristics where a large portion of the bedrock is granite (Sharma et al., 1999; Defence Science and Technology Agency (DSTA), 2009). Drill-and-blast method is the most widely used method for large-scale rock breaking activities in civil engineering construction due to its cost effectiveness, higher efficiency and ability to break hard rock (Jhanwar et al., 2000; Bossart et al., 2002; Onederra et al., 2012).

In a blasting operation, the main function of explosives is to break the rocks by releasing a large amount of energy. However, only a portion of the energy is consumed in breaking the rocks and the remaining energy is dissipated in the form of seismic waves expanding rapidly outward from the blast as ground vibrations and

air blast (Hagan, 1979; Lopez-Jimeno et al., 1995; Khandelwal and Singh, 2007; Kuzu, 2008). Ground vibrations from rock blasting are a particular concern as the vibration which has high amplitude and short duration can cause damage to nearby structures. In practice, the damage to nearby structures due to ground vibrations is controlled by the building authorities through various rules and regulations such as limiting the peak particle velocity (PPV). However, these vibration limits are not always valid, as they depend on the site-specific geological conditions and the dynamic characteristics of the structure. Structural responses to ground vibrations from blasting have been extensively studied with the objective to determine safe vibration limits. Duvall and Fogelson (1962), Wiss (1968), Nicholls et al. (1971) and Wiss and Nicholls (1974) concluded that blast-induced damage to residential structures is dependent on the ground particle velocity and the dominant frequency. Various national guidelines associating the threshold of visible damage to buildings with the PPVs have been proposed (BS 3785-1, 1990; ISO 4866, 1990; DIN 4150-3, 1999). Most countries use these regulations to keep the vibration level of ground and structures within a specific limit. However, there are no universal vibration limits that can cover all varieties of structures and geological conditions across various countries.

A number of researchers have investigated the problem of ground vibration prediction and have proposed various formulae

* Corresponding author.

E-mail address: CZZHAO@ntu.edu.sg (Z. Zhao).

Peer review under responsibility of Institute of Rock and Soil Mechanics, Chinese Academy of Sciences.

<https://doi.org/10.1016/j.jrmge.2018.12.009>

1674-7755 © 2019 Institute of Rock and Soil Mechanics, Chinese Academy of Sciences. Production and hosting by Elsevier B.V. This is an open access article under the CC BY-NC-ND license (<http://creativecommons.org/licenses/by-nc-nd/4.0/>).

(Langefors and Kihlstrom, 1978; Wiss, 1982; Zhou et al., 1998; Kumar et al., 2016). These formulae were obtained based on field observations from various sites. According to Siskind et al. (1980), amplitudes, frequencies and durations of the ground vibrations change during wave propagation due to various factors such as geometric absorption and interaction with various geological media and structural interfaces. Zhou et al. (1998) experimentally studied the ground shock wave propagation through mixed geological media due to detonation of explosive in an underground storage chamber. Kahriman (2004) carried out field tests at a limestone quarry to establish a reliable formula to predict the PPV. Field tests are very expensive and time-consuming due to extensive instrumentation and coordination. Thus, with the rapid development of detonation and rock interaction theory and computer technology, numerical simulation has become a promising method to understand the rock blasting process (Esen, 2008; Saharan and Mitri, 2008; Mitelman and Elmo, 2014; Jayasinghe et al., 2017). Onederra et al. (2012) developed a hybrid stress blasting model (HSBM) which combines continuous and discontinuous numerical techniques to model detonation, wave propagation, rock fragmentation, and muck pile formation. This model is capable of predicting the extent and shape of blast-induced damage zone with an adequate accuracy. Wu et al. (2004) numerically studied the ground wave propagation through granite and proposed a formula to predict PPV attenuation in rock. Wei et al. (2009) investigated the damage depth into rock mass induced by underground explosion and PPV attenuation in Bukit Timah granite through numerical simulations using ANSYS LS-DYNA and the numerical model was calibrated using the experimental results.

The vibration caused by rock blasting is highly dependent on the blast design, as well as the ground geological condition and the distance from the blasting location to the location where the vibration is concerned (Nateghi, 2011). Study of blasting is especially significant to identify the adverse effects, thereby reducing the potential damage to nearby buildings and minimizing annoyance to neighboring residents. However, to date, there have been only limited studies on the impact of vibration generated by blasting in Singapore. Thus, a series of field tests was conducted at a location in the northwestern part of Singapore to establish the attenuation law of the rock blasting induced vibration along the ground surface and at various depths in the residual soil and rock. The other objective of this study was to investigate the effect of the soil-rock interface on the stress wave propagation. Accelerometers were employed at different standoff distances from the blasting, and the acceleration time-histories were recorded at the ground surface, at various depths in the soil, as well in the rock mass to monitor the vibration.

In this paper, a brief description of the test layout and the instrumentation is presented first. Then, the measured results and the analyses of the PPV are presented and discussed.

2. Site geology and test setup

The test site is located in the northwestern part of Singapore. To study the characteristics of stress wave propagation and reflection along the rock-soil interface, a rectangular area of 70 m by 30 m with a downslope soil-rock interface was selected. The residential and commercial buildings are located far away from the test site. The nearest structure is a transport depot which is about 430 m away from the blasting area.

Before the field blast tests, soil investigations were carried out to establish the subsurface ground conditions. This involved 17 boreholes in which standard penetration tests (SPTs) and undisturbed soil sampling were carried out at 3 m interval. In addition, a cross-hole seismic tomography survey was carried out to verify the site geological conditions.

The ground conditions of the site consisted of medium-grained granite bedrock, overlain by residual soils (Zhao et al., 1994a, b). The rock-cores retrieved from the boreholes indicated the occurrence of Bukit Timah granite (Sharma et al., 1999). The completely weathered granite G(V) was composed of slightly gravelly fine-to-coarse sandy silt and this layer was observed in all the boreholes with thickness varying from 0.6 m to 11 m. The slightly weathered granite G(II) was encountered at depths of between 0.6 m and 11 m below the ground level.

Fig. 1 shows the cross-section of the test site, which shows a downward sloping soil-rock interface. In order to determine the PPV, it is necessary to measure the vibration in three orthogonal directions. Thus, triaxial accelerometers were used for the field vibration monitoring. The axes monitored by the accelerometers are longitudinal (radial), vertical and transverse. Two types of accelerometers (BnK 4520 and 4524 series) were used and they were designed for measuring high gravitational acceleration with inbuilt preamplifiers which operate over a frequency range of 2–7000 Hz and 0.25–3000 Hz, respectively.

In total, 14 triaxial accelerometers were employed at different standoff distances from the blast holes, as shown in Fig. 1. Accelerometers R1–R5 and S1–S5 were employed to measure the acceleration time-histories in rock and near the ground surface, respectively. In addition, four accelerometers (F1, F2, F3 and M1) were used to measure the free field ground shock at various soil depths. Table 1 shows the locations of the accelerometers. Locations of the blast holes (denoted by the notations B0, B1, etc.) are also

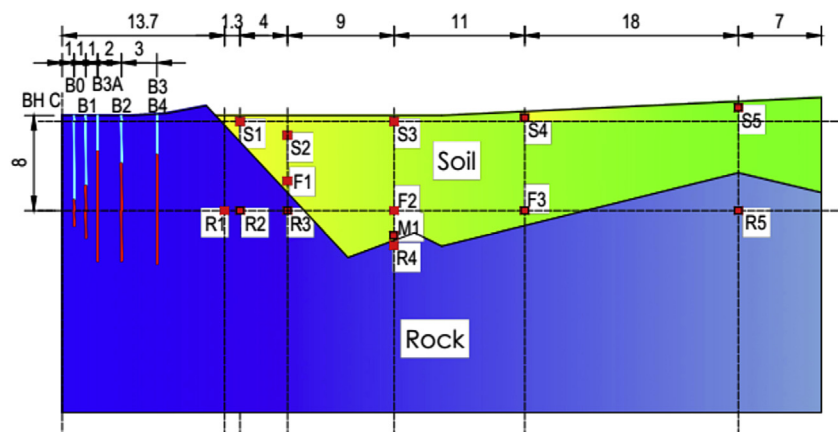


Fig. 1. Cross-section of the field test site (unit: m).

Table 1
Locations of accelerometers.

Sensor No.	Distance from BH C (m)	Depth below ground surface (m)
S1 (in soil)	15	0.5
S2 (in soil)	19	1.65
S3 (in soil)	28	0.5
S4 (in soil)	39	0.5
S5 (in soil)	57	0.5
R1 (in rock)	13.7	8
R2 (in rock)	15	8
R3 (in rock)	19	8
R4 (in rock)	28	10.7
R5 (in rock)	57	8
F1 (in soil)	19	5.5
F2 (in soil)	28	8
F3 (in soil)	39	8
M1 (in soil)	28	10.3

shown in Fig. 1. All the distances are measured from the reference borehole C (BH C), which was used in the soil investigations.

To accurately measure the ground vibration in rock, the measurement boreholes were drilled first. Then, an accelerometer was firmly installed inside a metal casing (metal penetrator), whose outer diameter is smaller than the measurement borehole, as shown in Fig. 2. Next, the accelerometer with the metal casing was attached to a long installation pipe to ensure the alignment of the accelerometer with the pipe. Later, the entire measurement setup was lowered into the borehole till it reached the specified depth. Then the installation pipe was removed by releasing the wire rope and leaving the accelerometer with the metal casing in the borehole. Subsequently, the measurement borehole was grouted to ensure that the casing was firmly set in place. This installation procedure was used to ensure that the accelerometers move together with the surrounding rock and accurately capture the free field vibration intensity. Installation of the accelerometers in rock is illustrated in Fig. 3.

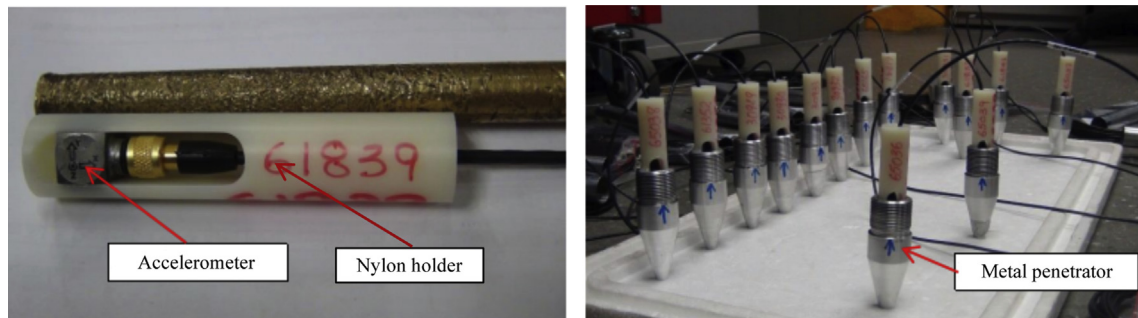


Fig. 2. Accelerometers firmly installed inside the metal casings.

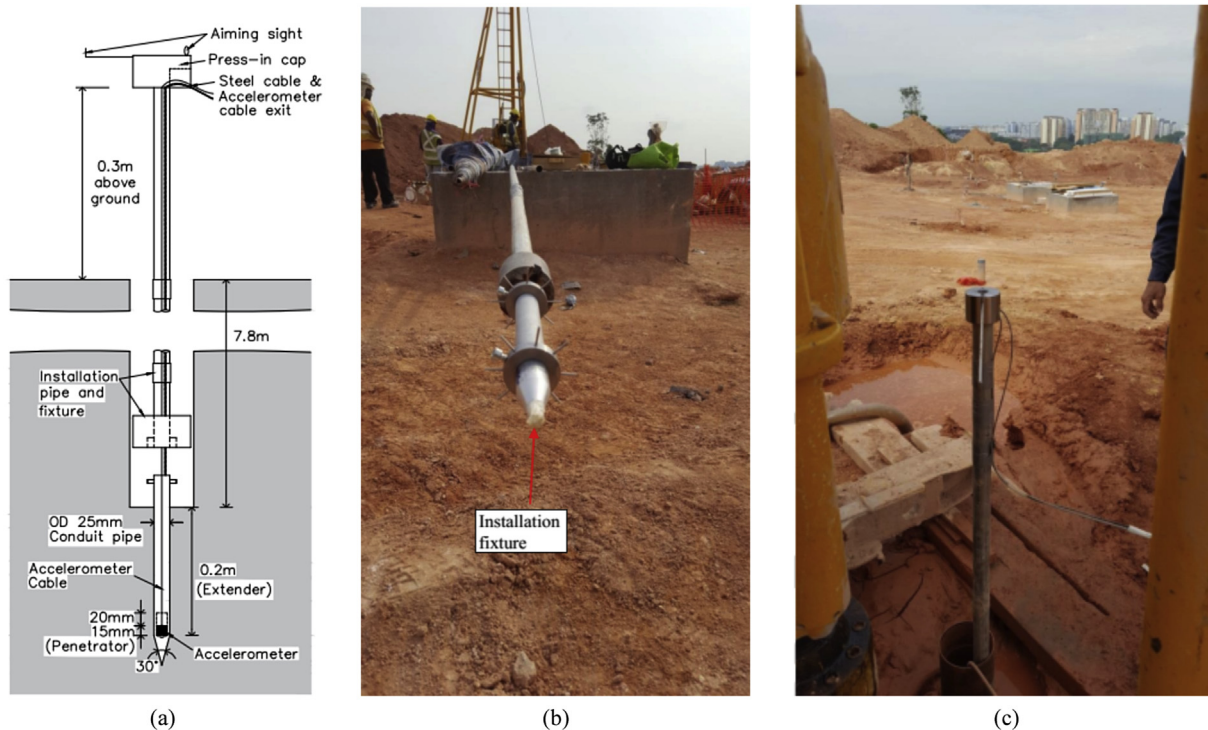


Fig. 3. Installation of accelerometers in rock: (a) Accelerometer fixture; (b) Accelerometer with the metal casing attached to an installation pipe; and (c) Ensuring the alignment of the sensor orientation.

Measuring the free field acceleration time-history in soil is challenging, since soil is relatively more flexible in terms of stiffness, thus the accelerometers cannot be rigidly (or relatively rigidly) attached. Proper installation is required to ensure that the time-history recorded by the accelerometers is not the response of the sensor itself, but the free field acceleration of the soil. For the installation of the surface sensors, the casings with accelerometers were directly pushed 0.5 m below the ground surface, with the aid of a pre-drilled guide hole. For the sensors in the soil, for example the sensors installed at 8 m below the ground surface, the measurement boreholes were drilled to 7.8 m depth and the casings with accelerometers were lowered into the hole. Then the casing was pushed 0.2 m deep and subsequently the hole was backfilled with soil. This installation procedure was used to ensure that the casings are in firm contact with the surrounding soil, which allows accurate measurement of the free field ground vibration. Installation of accelerometers in the soil is illustrated in Fig. 4.

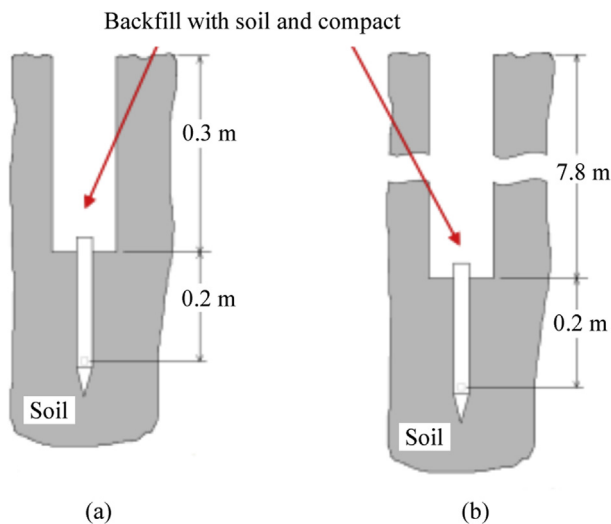


Fig. 4. Installation of accelerometers in the soil at (a) 0.5 m and (b) 8 m below ground surface.

Table 2
Summary of blast tests.

Blast test	Distance from BH C (m)	No. of blast holes	ANFO mass (kg)
B0	1	1	6.25
B1	2	1	12.5
B2	5	1	24
B3	8	2	58.1
B3A	3	3	84.9
B4	8	6	168.5

In total, six blasting tests were carried out, as summarized in Table 2. The first two blast tests (B0 and B1) were carried out to check and test the data logger's settings, and the remaining four blast tests (B2, B3, B3A and B4) were conducted to study the propagation and attenuation characteristics of the blast-induced vibrations on the ground surface, in the soil and rock. The sequence of the tests was B0, B1, B2, B3, B3A and B4, respectively. Each blast hole was 76 mm in diameter and the explosives used in the tests were ammonium nitrate-fuel oil (ANFO). The detonator used in the test was an electronic detonator. The middle of the ANFO charging columns in each hole was kept in a horizontal line, as illustrated in Fig. 1. Thus, the depths of the holes varied between 9.3 m and 12.9 m while stemming column and ANFO charging column heights were 2.8–7.1 m and 2.2–9.3 m, respectively. Stemming is the portion of blast hole which had been packed with gravel chips (less than 10 mm in size) above the charge so as to confine and retain the gases produced by the explosion, thus improving the fragmentation process.

3. Results and discussion

As described above, the measured ground vibrations in all the accelerometers from blast tests B2, B3, B3A and B4 were used to study the propagation and attenuation characteristics of blast-induced vibration on the ground surface, in the soil and rock. The PPV attenuation laws for blast-induced vibration on the ground surface, in the soil and rock, were developed and the wave strengthening and weakening effects due to wave reflection along the soil-rock interface were investigated by analyzing the relationships between PPV and scaled distance (SD), where SD is calculated by dividing distance from blasting point to vibration measurement point (D) by the square root of charge weight (W).

3.1. Ground vibration data

Acceleration time-histories in three directions (longitudinal, vertical and transverse) were monitored for each blast. Then, the velocity time-histories were obtained by numerically integrating the acceleration time-histories after a baseline correction and PPV values were calculated as the vector sum of three velocity components evaluated at the same time. Fig. 5 shows a sample of the recorded acceleration time-history at R1 in the longitudinal direction for blast test B2, and the corresponding calculated velocity time-history is shown in Fig. 6.

Figs. 7 and 8 show the calculated velocity time-histories in the vertical direction at R4, just below the soil-rock interface, and at M1, just above the soil-rock interface, respectively, calculated during blast test B2. Very high frequency components of the stress wave attenuate very quickly when it propagates in the soil mass.

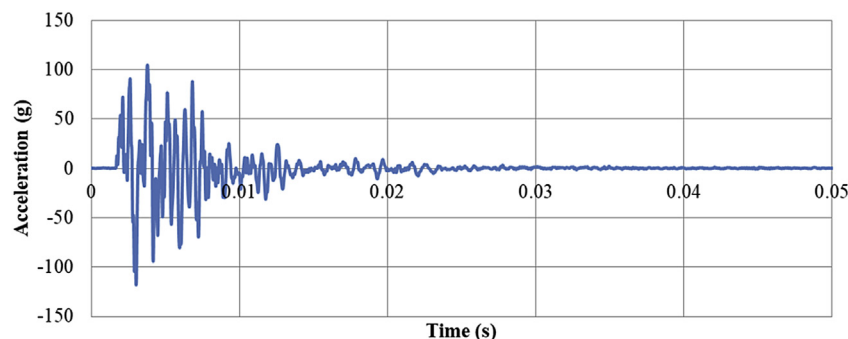


Fig. 5. Measured acceleration at R1 in the longitudinal direction for blast test B2.

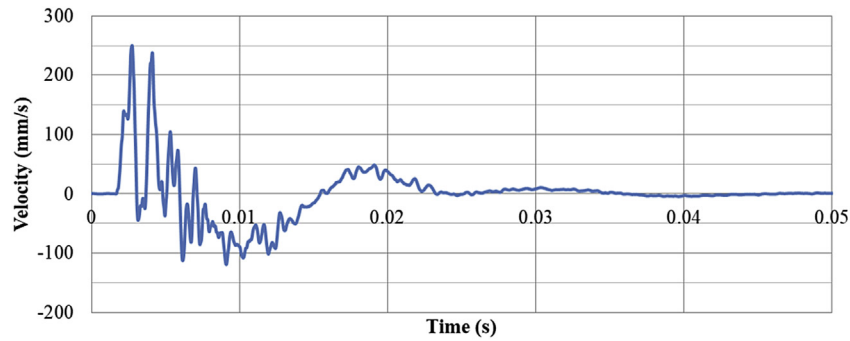


Fig. 6. Velocity time-history at R1 in the longitudinal direction for blast test B2.

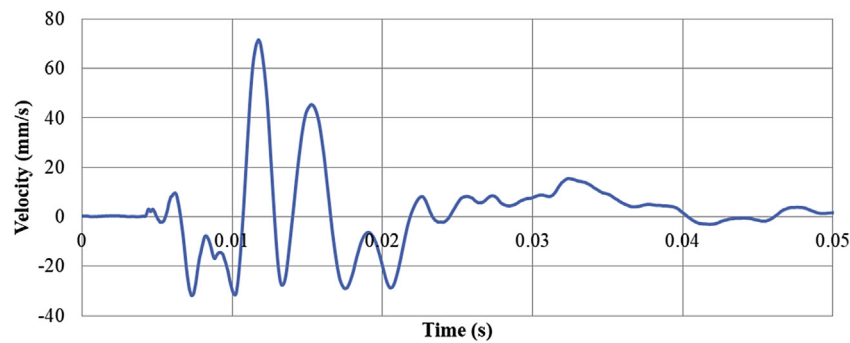


Fig. 7. Velocity time-history at R4 in the vertical direction for blast test B2.

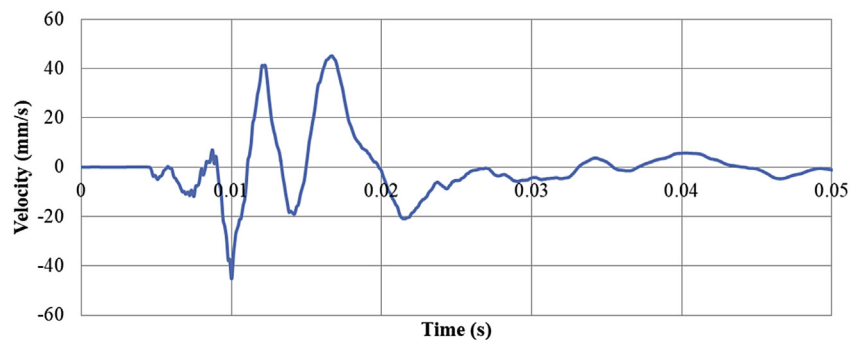


Fig. 8. Velocity time-history at M1 in the vertical direction for blast test B2.

The results indicate that the stress wave inside the soil mass (at M1) has a significantly smaller amplitude compared to that inside the rock mass (at R4).

The calculated PPV values at each monitoring point for each blast are presented in Table 3. The accelerometers at monitoring points S5 and F1 had poor signals in the vertical direction while the accelerometer at M1 had poor signals in the longitudinal direction for all of the blast tests. The accelerometers at monitoring points R1 and R4 had poor signals in all three directions for blast tests B3A and B4 and B3 to B4 tests, due to that the sensors were damaged during and/or after the installation. Thus, the PPV values were not computed for those corresponding points as tabulated in Table 3.

3.2. PPV attenuation at ground surface

The calculated PPV values at monitoring points S1, S3, S4 and S5 were used to study the PPV attenuation along the ground surface.

The test data include the charge weight (W), distance from blasting point to vibration measurement point (D), and PPV values at those monitoring points. The plotted graphs between PPV and SD for each blast test are shown in Fig. 9.

It can be clearly seen that the attenuation coefficient values are different for each test, mainly due to the down-slope soil-rock interface. The interface can affect the wave attenuation significantly, for both the PPV and the attenuation trend. The cracks developed from the previous blast may also possibly have some influence on the blast energy dissipation and wave propagation.

All the PPV values at ground surface were plotted against SD in log scale, as shown in Fig. 10. The ground vibration attenuation equation of the relation between the PPV and SD, with coefficient of determination (R^2), is shown in Fig. 10.

The empirical PPV attenuation law along the ground surface can be fitted by Eq. (1) with the coefficient of determination (R^2) of 0.8586:

Table 3
PPV values at the monitoring points.

Monitoring point	PPV (mm/s)			
	B2	B3	B3A	B4
S1	164.1	332.6	212.4	363.9
S2	68.5	139.7	90.4	179.2
S3	33.1	71.46	62.85	71.76
S4	22.2	35.5	36.19	37.73
S5				
F1				
F2	57.1	122.7	80.6	112.1
F3	21.3	31.25	36.38	39.93
M1				
R1	254	558		
R2	223	358	226	371
R3	182	332	216	592
R4	85			
R5	12.6	19.31	21.14	15.9

$$PPV = 210.76(SD)^{-1.223} \quad (1)$$

3.3. PPV attenuation in soil

Accelerometers S2 and F1 were installed in the soil at 1.65 m and 5.5 m below the ground surface, respectively, to study the ground vibration attenuation in the soil at different depths. Unfortunately, the PPV at F1 could not be determined as the accelerometer F1 had a poor signal in the vertical direction. Hence, the outputs from the accelerometer at the monitoring point S2, which is located in soil 1.65 m below the ground surface, were used to study the PPV attenuation in the residual soil. The empirical relationship between SD and PPV is plotted in Fig. 11 and the fitting curve can be expressed in Eq. (2) with $R^2 = 0.9254$:

$$PPV = 161.91(SD)^{-0.826} \quad (2)$$

3.4. PPV attenuation at 8 m depth below the ground surface

As shown in Fig. 1, a total of six accelerometers were installed at 8 m below the ground surface with four sensors (R1, R2, R3 and R5) in rock and two sensors (F2 and F3) in soil. The outputs from each accelerometer were used to study the PPV attenuation at 8 m depth below the ground surface and to investigate the effects of the soil-rock interface on the PPV attenuation trends.

The plotted graphs between PPV and SD for each test are presented in Fig. 12. At 8 m depth, the rock–soil interfaces were found just after the monitoring point R3 and between the monitoring points F3 and R5. The vertical red lines in the figure indicate the soil-rock interface locations at 8 m depth. When comparing the PPV in the rock (R1–R3) and in the soil (F2 and F3), it is clear that the wave attenuation in rock is much slower than that in the soil. Fig. 12 shows that the soil-rock interface plays a significant role in the blast wave propagation. The PPV value declines drastically after the soil-rock interface. It can also be clearly seen that the PPV attenuation laws are different for each test. As stated above, this is mainly due to the wave strengthening and weakening effect due to wave reflection along the soil-rock interface and possibly the blast energy dissipation through the cracks developed during the previous blasts.

All the PPV values calculated at 8 m depth below the ground level were plotted in Fig. 13. The obtained empirical equation from the graph for ground vibration attenuation which correlates the PPV and SD (with coefficient of determination of 0.8191) is shown as

$$PPV = 337.18(SD)^{-1.433} \quad (3)$$

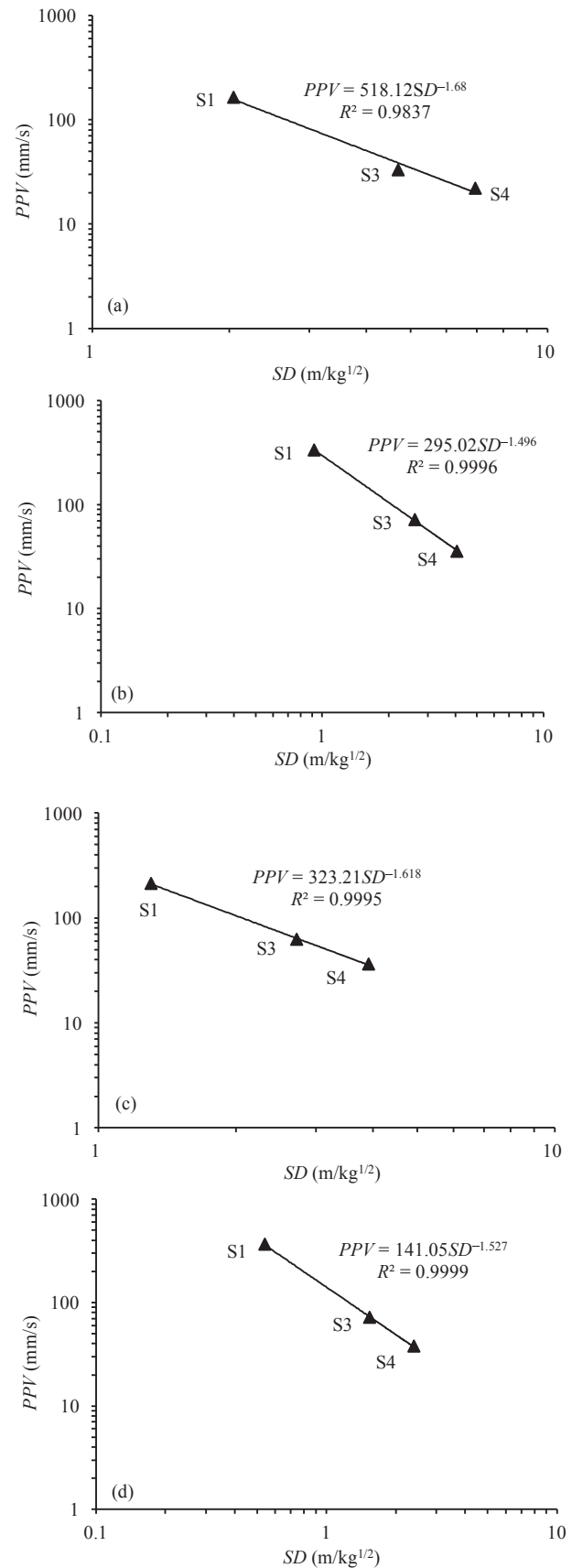


Fig. 9. PPV attenuation along the ground surface for blast tests (a) B2, (b) B3, (c) B3A, and (d) B4.

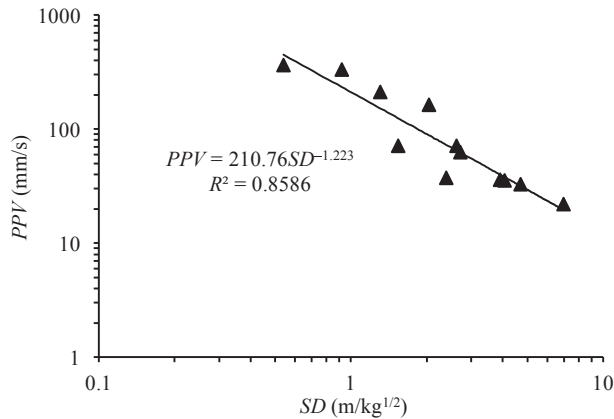


Fig. 10. PPV attenuation along the ground surface combining all field tests.

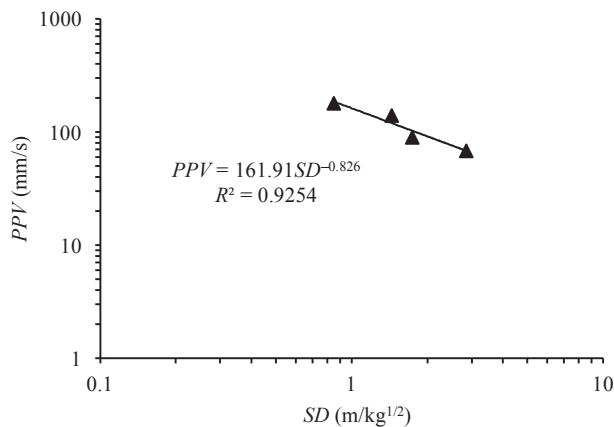


Fig. 11. PPV attenuation in the soil at 1.65 m below the ground surface.

Fig. 14 compares the blast wave attenuation on the ground surface and at depth of 8 m below the ground surface. The red dashed line and blue line represent the PPV attenuation trends at 8 m depth below the ground surface and on the ground (soil) surface, respectively. It is noted that the PPV values at 8 m depth below the ground surface are higher than those at ground surface in the near field. However, when the distance from the blast hole increases, the blast wave attenuates faster in deeper level than that on the ground surface. For blast test B4, when the scaled distance is greater than $2.54 \text{ m/kg}^{1/2}$, i.e. the distance from the blast hole is greater than 33 m, the PPV on the ground surface is much higher than that at 8 m depth below the ground surface. This is due to that the body waves are predominant at the near field and they decrease with the distance from the vibrating source. On the other hand, the intensities of surface waves are higher at the far field when comparing with the body waves. The measured results revealed that PPV attenuation rate is quite different at the ground surface and at different depths from the ground surface.

Moreover, in order to understand the stress wave distribution along the vertical direction, four accelerometers (S3, F2, M1 and R4) were installed at different depths from the ground surface at 28 m distance away from the BH C. As discussed above, accelerometer S3 was located just below the ground surface and it was used to measure the stress wave propagation on the ground surface while accelerometer F2 was used to measure the stress wave propagation at 8 m depth in soil mass. The accelerometers M1 and R4 were installed just above and below the soil-rock interface, respectively. Since the accelerometer M1 had poor signals in the longitudinal

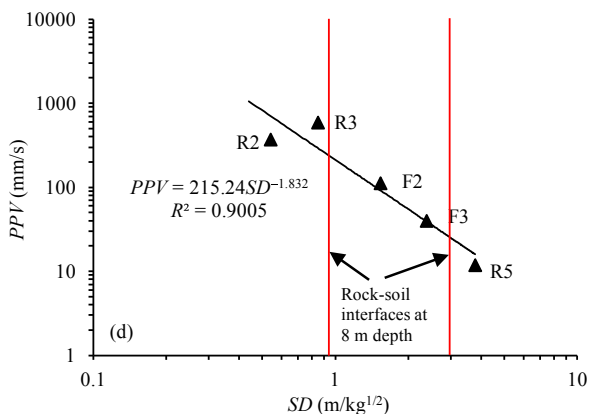
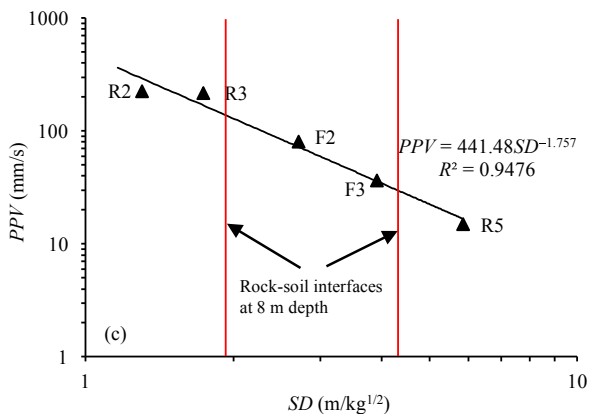
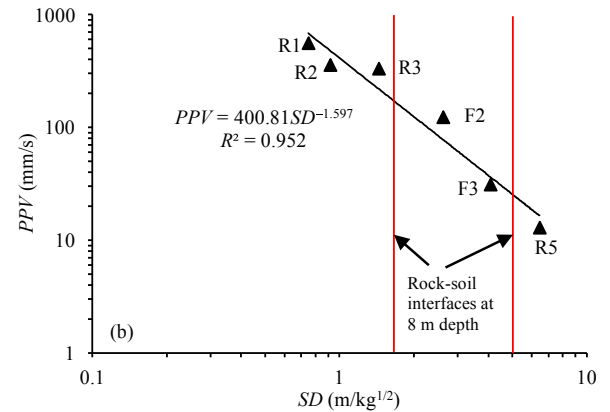
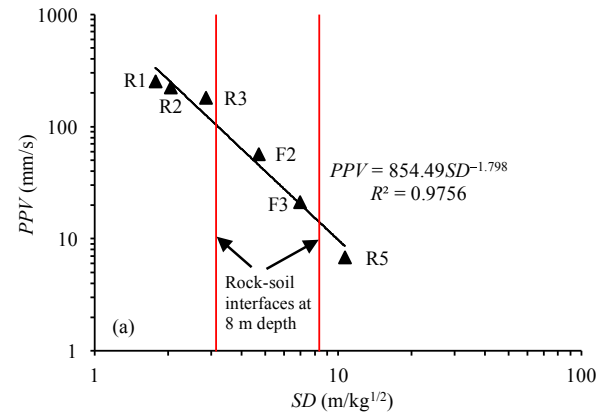


Fig. 12. PPV attenuation at depth of 8 m for blast tests (a) B2, (b) B3, (c) B3A and (d) B4.

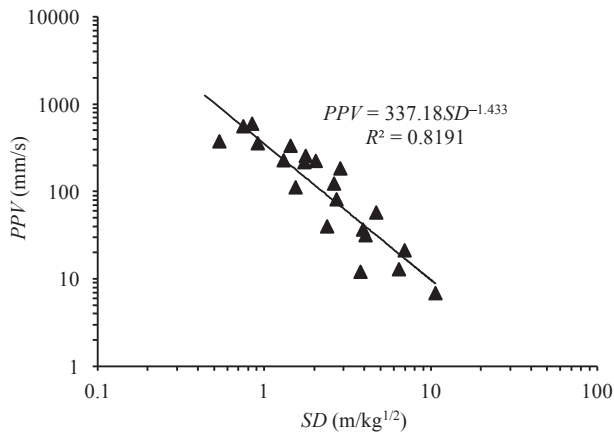


Fig. 13. PPV attenuation at 8 m depth combining all field tests.

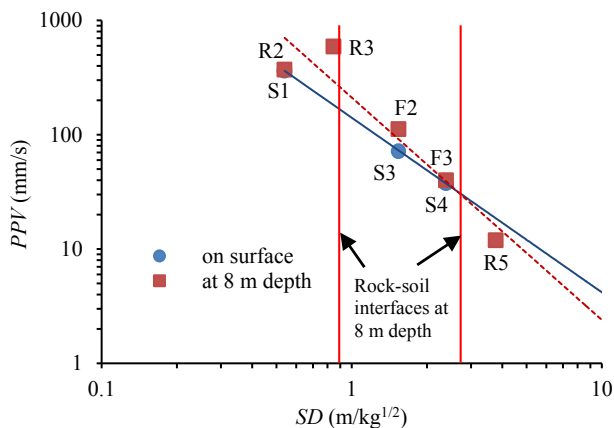


Fig. 14. Comparison of PPV attenuation at ground surface and depth of 8 m for blast test B4.

direction, the PPV distribution along the vertical direction cannot be compared. Hence, the peak velocities in the vertical direction were used to compare stress wave distribution along the vertical direction. Fig. 15 shows the stress wave distribution along the vertical direction for blast test B2. It can be seen that the ground vibration on the ground (soil) surface is much smaller when comparing to that in the soil mass as well as in the rock mass. Also, stress wave inside the soil mass is smaller compared to the stress

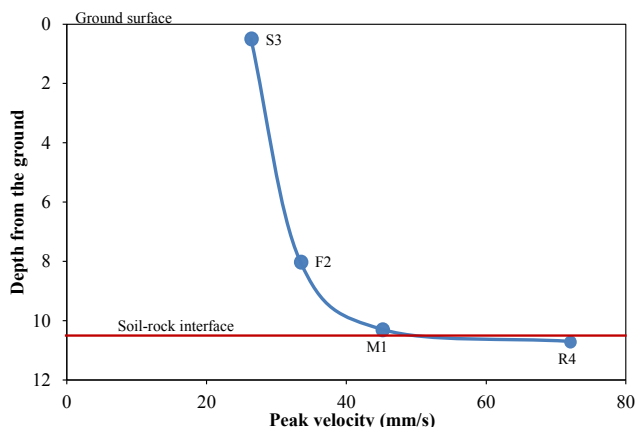


Fig. 15. Stress wave distribution along the vertical direction for blast test B2.

wave inside the rock mass as the stress wave attenuates very quickly when propagating across the soil-rock interface. Since the PPV on the ground surface can be smaller than that below the ground surface, it may not be suitable to use the ground surface measurement to assess the safety of the underground structures under rock blasting induced vibration.

4. Conclusions

This paper summarized the field test results from a series of blasting tests conducted at a site with residual soil overlying granitic rock in Singapore. A downward sloping soil-rock interface existed at the test area. Triaxial accelerometers were used to measure the free field acceleration time-histories on the ground surface, at various depths in the soil layer and in the rock.

This research developed the PPV attenuation laws for blast-induced vibration on ground surface and at various depths below the ground level. It was found that the PPV attenuation trend varies with the change of the geological conditions. Even at the same site, PPV estimation can be quite different at different locations/directions. Thus, it is recommended that blasting contractors should provide direction-based PPV attenuation prediction formulae, and update the formulae at different excavation stages as variations in geological profile (as excavation is sequentially carried out) can change the PPV attenuation significantly.

It was also found that PPV on the ground surface can be significantly smaller than that below the ground surface, thus it may not be suitable to use the ground surface measurement to assess the safety of the underground structures (such as foundation and pipeline) under rock blasting induced vibration.

Also, the ground vibration attenuation across the soil-rock interface was carefully examined and the study shows that the soil-rock interface plays a significant role in reducing the ground vibration intensity. It is recommended that for blasting site with a close range soil/rock interface, further field tests and/or numerical simulations are needed, in order to understand the potential amplification of PPV due to the soil-rock interface.

Conflicts of interest

The authors wish to confirm that there are no known conflicts of interests associated with this publication and there has been no significant financial support for this work that could have influenced its outcome.

Acknowledgements

This article is based on research work supported by the Land and Liveability National Innovation Challenge under L2 NIC Award No. L2NICFP1-2013-1. Any opinions, findings, and conclusions or recommendations expressed in this material are those of the authors and do not necessarily reflect the views of the L2 NIC. Assistance during the field tests given by the staff from JTC Corporation, Chye Joo Construction Pte. Ltd., Asia Tunnelling and Construction Pte. Ltd., and Singapore Test Services is gratefully acknowledged.

References

- Bossart P, Meier PM, Moeri A, Trick T, Mayor JC. Geological and hydraulic characterisation of the excavation disturbed zone in the Opalinus clay of the Mont Terri rock laboratory. *Engineering Geology* 2002;66(1):19–38.
- BS 7385-1. Evaluation and measurement for vibration in buildings. British Standards Institution (BSI); 1990.
- Defence Science and Technology Agency (DSTA). *Geology of Singapore*. 2nd ed. Singapore: DSTA; 2009.

- DIN 4150-3. Structural vibration — effects of vibration on structures. German Institute for Standardization (DIN); 1999.
- Duvall WI, Fogelson DE. Review of criteria for estimating damage to residences from blasting vibrations. Report of investigation 5968. US bureau of Mines; 1962.
- Esen S. A non-ideal detonation model for evaluating the performance of explosives in rock blasting. *Rock Mechanics and Rock Engineering* 2008;41(3):467–97.
- Hagan TN. Rock breakage by explosives. *Acta Astronautica* 1979;6(3–4):329–40.
- ISO 4866. Mechanical vibration and shock — vibration of buildings — guidelines for the measurement of vibrations and evaluation of their effects on structures. International Organization for Standardization (ISO); 1990.
- Jayasinghe LB, Zhou HY, Goh ATC, Zhao ZY, Gui YL. Pile response subjected to rock blasting induced ground vibration near soil-rock interface. *Computers and Geotechnics* 2017;82:1–15.
- Jhanwar JC, Jethwa JL, Reddy AH. Influence of air-deck blasting on fragmentation in jointed rocks in an open-pit manganese mine. *Engineering Geology* 2000;57(1):13–29.
- Kahrman A. Analysis of parameters of ground vibration produced from bench blasting at a limestone quarry. *Soil Dynamics and Earthquake Engineering* 2004;24:887–92.
- Khandelwal M, Singh TN. Evaluation of blast-induced ground vibration predictors. *Soil Dynamics and Earthquake Engineering* 2007;27(2):116–25.
- Kumar R, Choudhury D, Bhargava K. Determination of blast-induced ground vibration equations for rocks using mechanical and geological properties. *Journal of Rock Mechanics and Geotechnical Engineering* 2016;8(3):341–9.
- Kuzu C. The mitigation of the vibration effects caused by tunnel blasts in urban areas: a case study in Istanbul. *Environmental Geology* 2008;54:1075–80.
- Langefors U, Kihlstrom B. The modern techniques of rock blasting. 3rd ed. New York: Wiley; 1978.
- Lopez-Jimeno C, Lopez-Jimeno E, Carcedo A. Drilling and blasting of rocks. New York: Taylor & Francis; 1995.
- Mitelman A, Elmo D. Modelling of blast-induced damage in tunnels using a hybrid finite-discrete numerical approach. *Journal of Rock Mechanics and Geotechnical Engineering* 2014;6(6):513–22.
- Nateghi R. Prediction of ground vibration level induced by blasting at different rock units. *International Journal of Rock Mechanics and Mining Sciences* 2011;48(6):899–908.
- Nicholls HR, Johnson FJ, Duvall WL. Blasting vibrations and their effects on structures. Washington, D.C.: Bureau of Mines; 1971.
- Onederra IA, Furtney JK, Sellers E, Iverson S. Modelling blast induced damage from a fully coupled explosive charge. *International Journal of Rock Mechanics and Mining Sciences* 2012;58(4):73–84.
- Saharan MR, Mitri HS. Numerical procedure for dynamic simulation of discrete fractures due to blasting. *Rock Mechanics and Rock Engineering* 2008;41(5):641–70.
- Sharma JS, Chu J, Zhao J. Geological and geotechnical features of Singapore: an overview. *Tunnelling and Underground Space Technology* 1999;14(4):419–31.
- Siskind DE, Stagg MS, Kopp JW, Dowding CH. Structure response and damage produced by ground vibration from surface mine blasting. Report of Investigation 8507. Washington, D.C.: Bureau of Mines; 1980.
- Wei XY, Zhao ZY, Gu J. Numerical simulations of rock mass damage induced by underground explosion. *International Journal of Rock Mechanics and Mining Sciences* 2009;46(7):1206–13.
- Wiss JF. Effect of blasting vibrations on buildings and people. *Civil Engineering* 1968;38(7):46–8.
- Wiss JF. Construction vibrations: state of the art. *Journal of Geotechnical Engineering* 1982;107(2):167–81.
- Wiss JF, Nicholls HR. A study of damage to a residential structure from blast vibrations. The Research Council for the performance of structures. American Society of Civil Engineers (ASCE); 1974.
- Wu C, Lu Y, Hao H. Numerical prediction of blast-induced stress wave from large-scale underground explosion. *International Journal for Numerical and Analytical Methods in Geomechanics* 2004;28:93–109.
- Zhao J, Broms BB, Zhou Y, Choa V. A study of the weathering of the bukit timah granite, part A: review, field observations and geophysical survey. *Bulletin of the International Association of Engineering Geology* 1994a;49(1):97–105.
- Zhao J, Broms BB, Zhou Y, Choa V. A study of the weathering of the Bukit Timah granite, Part B: field and laboratory investigations. *Bulletin of the International Association of Engineering Geology* 1994b;50(1):105–11.
- Zhou YH, Chong KOY, Wu YK. Small-scale testing on ground shock propagation in mixed geological media. In: Proceedings of the 28th DOD explosives safety seminar; 1998.



Zhiye Zhao is an Associate Professor from the School of Civil and Environmental Engineering, Nanyang Technological University (NTU), Singapore, and the Director of the Nanyang Centre for Underground Space, NTU. He is a member of the editorial board of *Tunnelling and Underground Space Technology*, and *Journal of Rock Mechanics and Geotechnical Engineering*, and currently the President of the Society for Rock Mechanics & Engineering Geology (Singapore). His research focuses on the area of numerical modeling in rock mechanics/engineering, including development of the discontinuous deformation analysis (DDA), the rockbolt modeling, the rock cavern response under dynamic/blast loads, the coupled hydro-mechanical modeling and rock grouting simulations.